Peptide modified nanocarriers for selective targeting of bombesin receptors

Antonella Accardo,[a] Rosalba Mansi,[b] Anna Morisco,[a] Gaetano Mangiapia,[c] Luigi Paduano,[c] Diego Tesauro,[a] Aurel Radulescu,[d] Michela Aurilio,[e] Luigi Aloj,[e] Claudio Arra[f] and Giancarlo Morelli†*[a]

Received 5th November 2009, Accepted 22nd December 2009
First published as an Advance Article on the web 9th February 2010
DOI: 10.1039/b923147a

The present work describes new supramolecular aggregates obtained by co-assembling two different amphiphilic molecules, one containing the bioactive bombesin peptide (BN), or a scramble sequence, and the other, the DOTA chelating agent, $(C18)_2$DOTA, capable of forming stable complexes with the radioactive ^{111}In(III) isotope. The peptide in the amphiphilic monomer is spaced by the lipophilic moiety through ethoxylic spacers of different length: a shorter spacer with five units of dioxoethylene moieties in $(C18)_2$L5-peptide, or a longer spacer consisting of a Peg3000 residue in $(C18)_2$Peg3000-peptide. Structural characterization by SANS and DLS techniques indicates that, independently from the presence of the peptide containing monomer in the final composition, the predominant aggregates are liposomes of similar shape and size with a hydrodynamic radius R_h around 200 nm and bilayer thickness, d, of 4 nm. *In vitro* data show specific binding of the ^{111}In-$(C18)_2$DOTA/$(C18)_2$L5-[*7-14*]BN 90 : 10 liposomes in receptor expressing cells. However, the presence of the Peg3000 unit on the external liposomal surface, could hide the peptide and prevent the receptor binding. *In vivo* experiments using ^{111}In-$(C18)_2$DOTA/$(C18)_2$L5-[*7-14*]BN show the expected biological behavior of aggregates of such size and molecular composition, moreover there is an increase in concentration of the GRPR targeting aggregate in the tumors compared to control at the 48 h time point evaluated (2.4% ID/g *versus* 1.6% ID/g).

1. Introduction

Multimodal supramolecular compounds that combine imaging and therapeutic capabilities are the focus of intensive research for applications in the growing field of nanomedicine.[1,2] They offer the prospect to increase diagnostic accuracy and therapeutic effectiveness, while minimizing side effects from treatment. Nanoparticles with a micellar or liposomal structure obtained by assembling amphiphilic compounds are promising candidates for such multifunctional therapeutic platforms, since these materials are conveniently synthesized, variably functionalized, and can be assembled to a range of sizes and compositions. They have high drug-loading capacity, biodegradability, prolonged circulation times, slow plasma clearance and controllable drug-release profiles. The hydrophobic core of micelles and the inner cavity of liposomes are carrier compartments able to accommodate large amounts of drug, while the shell, consisting of a brush-like protecting corona, stabilizes them in aqueous solutions.[3,4] Moreover micelles and liposomes can be functionalized on their external surface by introducing reporter molecules such as peptides or antibodies to achieve specific and selective delivery to target cells,[5,6] and they can also be modified with a fluorescent, paramagnetic or radioactive probe for their visualization and for diagnostic purposes.[7]

An effective way to prepare nanoparticles with a micellar or liposomal structure modified with a reporter compound on their surface and with a paramagnetic or radioactive probe is the mixed assembly of different monomers. We have recently developed micelles and liposomes acting as target selective MRI contrast agents,[8–11] or as target selective drug delivery systems.[12,13] They have been obtained by co-assembling two different amphiphilic molecules, one containing a bioactive peptide and the other a chelating moiety capable of forming stable complexes with the paramagnetic Gd(III) ion or with the radioactive ^{111}In(III) isotope. Following this strategy we have now developed new *thera-diagnostic* supramolecular aggregates that can potentially act as target selective drug delivery systems and imaging probes, thus coupling together *therapeutic* and

[a] *Department of Biological Sciences, CIRPeB, University of Naples "Federico II", & IBB-CNR, Via Mezzocannone 16, 80134 Naples, Italy. E-mail: gmorelli@unina.it; Fax: +39 081 2536642; Tel: +39 081 2536650*
[b] *Division of Radiological Chemistry, University Hospital Basel, Basel, Switzerland*
[c] *Department of Chemistry, University of Naples "Federico II" Via Cynthia, 80126 Naples, Italy*
[d] *Forschungszentrum Jülich – Jülich Centre for Neutron Science, LichtenbergerStrasse 1, D-85747 Garching, Germany*
[e] *Department of Nuclear Medicine Istituto Nazionale per lo Studio e la Cura dei Tumouri, Fondazione "G. Pascale", Via M. Semmola, 80131, Naples, Italy*
[f] *Department of Animal experimentation Istituto Nazionale per lo Studio e la Cura dei Tumouri, Fondazione "G. Pascale", Via M. Semmola, 80131, Naples, Italy*
† In honor of Professor Helmut Maecke's retirement.

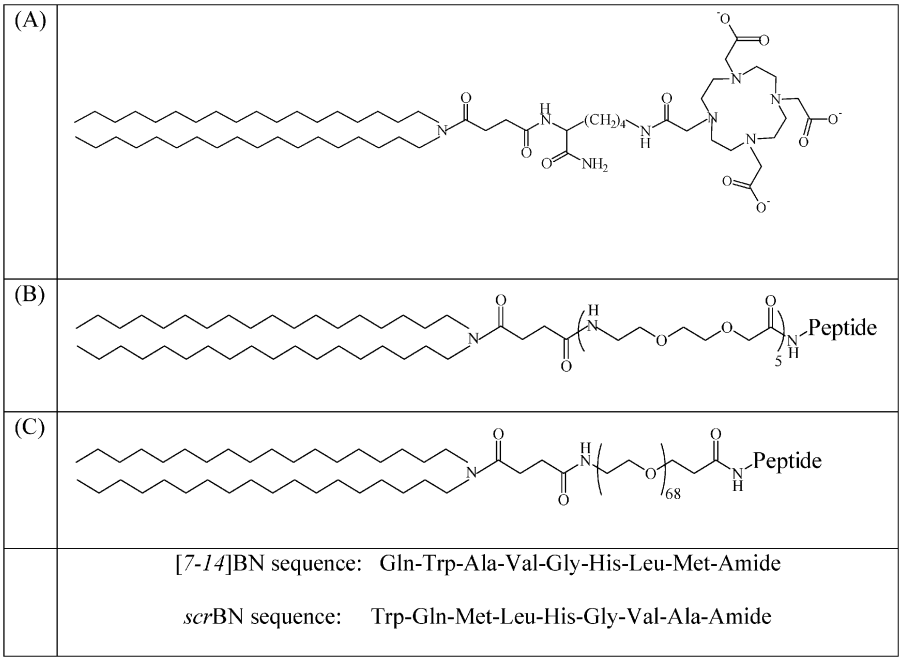

Fig. 1 Schematic representation of amphiphilic monomers: (A) $(C18)_2$DOTA; (B) $(C18)_2$L5-[7-*14*]BN or $(C18)_2$L5-*scr*BN(Sc); (C) $(C18)_2$Peg3000-[7-*14*]BN or $(C18)_2$Peg3000-*scr*BN.

diagnostic effectiveness. These new aggregates have been designed to target the members of the bombesin receptor family, which consists of four receptor subtypes including the neuromedin B receptor (BB1), the gastrin-releasing peptide receptor (GRPR, BB2), the orphan receptor subtype (BB3), and the amphibian receptor (BB4).[14–17]

The bombesin receptor subtype 2 (GRPR) has been found overexpressed by tumor cell lines of several human tumors (ovarian cancers, breast cancers and prostate cancer)[18–20] and thus it is indicated as a potential target for tumor diagnosis and selective therapy. The fourteen-residue bombesin peptide (BN), its eight-residue C-terminal peptide sequence ([7-*14*]BN), or some other bombesin analogue could act as antagonists and be used to target these receptors. Many studies have demonstrated that bombesin fragment [7-*14*]BN modified on the N-terminus with radiometal complexes for nuclear medicine applications preserves its affinity for these receptors.[21] Rogers and co-workers[22,23] evaluated the behavior of BN analogues containing aliphatic or amino acidic linkers placed between the BN peptide and the 1,4,7,10-tetraazacyclododecane-1,4,7,10-tetraacetic acid (DOTA) chelator. Results confirmed the target cell uptake with IC_{50} values in the nanomolar range in *in vitro* experiments and in *in vivo* studies.

In the present study, we report on new mixed supramolecular aggregates obtained by mixing the two amphiphilic monomers shown in Fig. 1. The more abundant monomer, used to drive the aggregation process, is the anionic surfactant $(C18)_2$DOTA, (monomer A in Fig. 1); it contains two C18 alkyl chains that allow the formation of supramolecular aggregates in water solution, a lysine residue acting as spacer, and the DOTA chelator. This cyclic chelating agent is able to coordinate radioactive metal ions such as $^{111}In(III)$ or $^{67/68}Ga(III)$, allowing the *in vivo* biodistribution of the aggregates to be followed by using nuclear medicine techniques.[24] The other, bioactive, amphiphilic monomer contains the same hydrophobic moiety with two C18 alkyl chains, and the bombesin analogue [7-*14*]BN. The peptide is spaced by the lipophilic moiety through ethoxylic spacers of different length. Two different spacers are used: a shorter spacer with five units of dioxoethylene moieties (monomer B, in Fig. 1) or a longer spacer consisting of a Peg3000 residue (monomer C in Fig. 1). The spacer performs several important tasks: it increases the peptide hydrophilicity; it distances the bioactive peptide from the surface of the supramolecular aggregate, thus giving a better peptide exposition and reducing potential hindrance to peptide binding activity; moreover it prevents the aggregates from being cleared through the reticulo-endothelial system (RES).[25] The *in vitro* and *in vivo* target selectivities of aggregates exposing the [7-*14*]BN peptide were compared with similar aggregates derivatized with a scrambled peptide, *scr*BN. The internalization rate of the ^{111}In labeled aggregates into PC-3 (human prostate cancer cell line) cells was studied and the pharmacokinetics of the more promising aggregate was evaluated in PC-3 tumor bearing nude mice.

2. Results and discussion

2.1 Monomers synthesis and aggregates preparation

The peptide conjugate DOTA-βAla-[7-*14*]BN, and the amphiphilic monomers $(C18)_2$L5-[7-*14*]BN and $(C18)_2$Peg3000-[7-*14*]BN were synthesized by Fmoc/*t*Bu chemistry according to standard solid phase peptide synthesis protocols, using Rink-amide MBHA resin as polymeric support.[26] The corresponding scrambled peptide compounds retaining the bombesin [7-*14*] amino acid residue composition, but with a reordered sequence, were prepared using similar procedures. As already

experienced with similar compounds the introduction of the Peg moiety or oxoethylene linkers was efficiently obtained by using the Fmoc-protected starting reagents (Fmoc-NH-Peg3000-COOH and five Fmoc-AdOO-OH, respectively), using a two-fold molar excess in the solid-phase synthesis protocols and PyBop/HOBt as activators. Also the hydrophobic *N*,*N*-dioctadecylsuccinamic acid was efficiently bound in solid-phase in a DMF–DCM mixture. All the peptide conjugates were collected in good yields after HPLC-RP chromatography purification. Analytical liquid chromatography mass spectrometry (LC-MS) data confirmed the compound identities and their high purity. $(C18)_2$DOTA anionic surfactant was crystallized by adding water drop-wise to the TFA cleavage solution and used without further purification. The identity of the product was confirmed by ESI MS and by NMR spectroscopy (^{1}H and ^{13}C). Pure aggregates of $(C18)_2$DOTA monomer, and mixed supramolecular aggregates containing the $(C18)_2$DOTA monomer and $(C18)_2$DOTA/$(C18)_2$L5-[*7-14*]BN or $(C18)_2$DOTA/$(C18)_2$Peg3000-[*7-14*]BN (or the aggregates containing the corresponding scrambled sequences) were prepared in 90 : 10 molar ratio in phosphate buffer at pH 7.4 following well known procedures.

2.2 Structural characterization

Fig. 2 shows the scattering cross sections collected for the binary aqueous systems $(C18)_2$DOTA and for the ternary aqueous systems $(C18)_2$DOTA/$(C18)_2$L5-[*7-14*]BN. In Fig. 3, examples of distribution functions obtained for hydrodynamical radii by means of DLS measurements are reported for aqueous systems $(C18)_2$DOTA, $(C18)_2$DOTA/$(C18)_2$L5-[*7-14*]BN and $(C18)_2$DOTA/$(C18)_2$Peg3000-[*7-14*]BN. Inspection of Fig. 2, reveals that, for both systems, the scattering cross sections $d\Sigma/d\Omega$, at high q, show a power low (q^{-2}) typical of bi-dimensional objects.

Actually, as also shown by DLS, this scattering behavior can be ascribed to the presence of large liposomal aggregates, whose Guinier regime falls almost completely in the very low

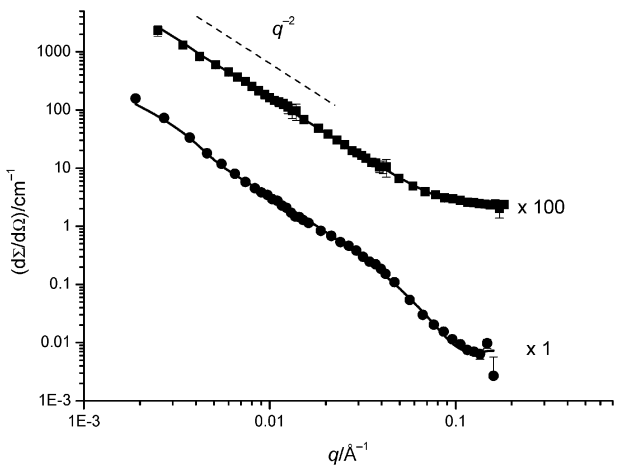

Fig. 2 Scattering cross sections at 25 °C of $(C18)_2$DOTA/D_2O (■) and $(C18)_2$DOTA/$(C18)_2$L5-[*7-14*]BN/D_2O (●). For a better visualization, data have been multiplied by a scaling factor as indicated. Curves obtained through the fitting of eqn (1) are also reported.

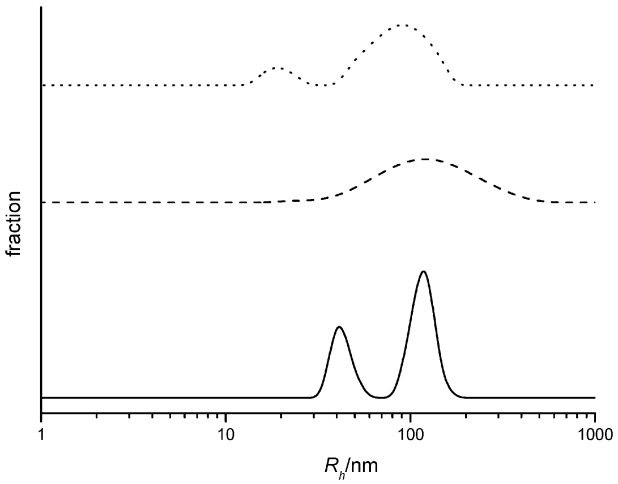

Fig. 3 Hydrodynamical radius distribution function obtained at 25 °C by means of DLS measurements for the following systems: $(C18)_2$DOTA/H_2O (—), $(C18)_2$DOTA/$(C18)_2$L5-[*7-14*]BN/H_2O (---) and $(C18)_2$DOTA/$(C18)_2$Peg3000-[*7-14*]BN/H_2O (····).

q value, undetectable with the SANS apparatus used. Thus, the aggregates presented in our systems have been modeled as a collection of randomly oriented planar sheets, for which the scattering cross sections can be expressed as

$$\frac{d\Sigma}{d\Omega} = 2\pi(\Delta\rho)^2 S d^2 \frac{1}{q^2}\frac{\sin^2\left(\frac{qd}{2}\right)}{\left(\frac{qd}{2}\right)} + \left(\frac{d\Sigma}{d\Omega}\right)_{\text{incoh}} \qquad (1)$$

where $\Delta\rho$ is the scattering length density difference between the scattering aggregates and the solvent, d is the plane thickness, S is the total surface per unit volume and $(d\Sigma/d\Omega)_{\text{incoh}}$ represents the incoherent contribution to the scattering cross section, mainly due to the presence of hydrogen nuclei. From a fitting of eqn (1) to the experimental data it is possible to evaluate the thickness d of the liposome double layer for the system analyzed. These values are collected in Table 1 together with the values obtained from DLS experiments. Concerning this latter technique, the distribution function obtained for the hydrodynamic radii shows the presence of two diffusive modes for $(C18)_2$DOTA and $(C18)_2$DOTA/$(C18)_2$Peg3000-[*7-14*]BN aqueous systems, whereas a single mode is present for the $(C18)_2$DOTA/$(C18)_2$L5-[*7-14*]BN system. The experimental self-diffusion coefficients D, obtained through the regularized inverse Laplace transformation of the correlation functions, are collected in Table 1. In the approximation of very diluted solutions, the data can be directly related to the hydrodynamic radii (see Table 1) of the aggregates, R_h, through the Stokes–Einstein equation, which holds for non-interacting hard spheres diffusing in a continuous medium. The sizes obtained for the aggregates formed by the synthesized molecules are consistent with the dimensions of micelles and liposomes, that coexist for $(C18)_2$DOTA and $(C18)_2$DOTA/$(C18)_2$Peg3000-[*7-14*]BN aqueous systems, whereas for the $(C18)_2$DOTA/$(C18)_2$L5-[*7-14*]BN system only large aggregates (liposomes) are present. However, in contrast with DLS results, the presence of micellar structures has not been detected in the SANS cross sections profile. It is worthy

Table 1 Liposomal bilayer thickness (d), translational diffusion coefficient (D) and hydrodynamical radius (R_h) obtained for the systems investigated by means of SANS and DLS

Aqueous system	d/Å	D/cm^2 s^{-1}	R_h/nm
$(C18)_2$DOTA	41 ± 2	(1.28 ± 0.07)10^{-8}	190 ± 11
		(5.0 ± 0.4) 10^{-8}	49 ± 4
$(C18)_2$DOTA/ $(C18)_2$L5-[*7-14*]BN	41 ± 6	(1.2 ± 0.1) 10^{-8}	200 ± 20
$(C18)_2$DOTA/	*n.m*[a]	(1.15 ± 0.04) 10^{-8}	211 ± 7
$(C18)_2$Peg3000-[*7-14*]BN		(1.15 ± 0.05) 10^{-7}	21 ± 2

[a] not measured.

to note that this circumstance does not imply the absolute absence of the smaller aggregates but can be ascribed to the ratio of the two populations that indicates a very large amount of liposomes, thus hiding the contribution of smaller micelles to the cross sectional scattering. By inspection of Table 1 it can be inferred that the thicknesses of the bilayers are fairly constant, around 41 Å, in the two analyzed systems. The low relative amount of the $(C18)_2$L5-[*7-14*]BN compared to the $(C18)_2$DOTA in the 10 : 90 mixed aggregates does not have a strong influence on the thickness of the double layers. Moreover the three supramolecular aggregates, independent of the presence of the peptide containing monomer in the final composition, show similar shapes and sizes with a hydrodynamic radius R_h around 200 nm. A schematic view of the liposomal aggregates is reported in Fig. 4.

As it concerns the micellar aggregates found, in low amount, in $(C18)_2$DOTA and $(C18)_2$DOTA/$(C18)_2$Peg3000-[*7-14*]BN samples, we note that DLS measurements are not able to provide the shape and the detailed dimensions of these objects. However, a simple calculation on the synthesized molecules, by assuming an all-*trans* conformation, provides a linear length of ~40–60 Å, quite far from the hydrodynamical radius found for the micellar structures, probably due to the formation of elongated structures like rod-like or worm-like micelles. Finally, SANS measurements carried out on mixed aggregates containing the monomer in which [*7-14*]BN peptide is replaced with the scrambled peptide sequence (*scr*BN), as expected, do not show significant structural modifications (data not shown).

2.3 *In vitro* studies

Binding and internalization assays of ^{111}In-DOTA-βAla-[*7-14*]BN and ^{111}In-DOTA-βAla-*scr*BN peptide conjugates were performed on PC-3 cell lines at 37 °C, at different time points (0.5, 1.0, 2.0 and 4.0 h), in order to confirm the effective binding capability of [*7-14*]BN and to evaluate if the peptide sequence chosen as scrambled peptide (*scr*BN) is an adequate negative control for the aggregate systems. Blocking studies performed using a large excess of [Tyr^4]-BN demonstrated that the uptake was receptor mediated. As shown in Fig. 5A, when incubating PC-3 cells with trace amounts of ^{111}In-DOTA-βAla-[*7-14*]BN, we found 8.98 ± 0.49% of the total amount of labeled peptide bound or was internalized at 4 h. This data is in agreement with previous reports in the literature[27] that show high affinity (IC_{50} of 2.1 ± 0.3 nM) binding of ^{111}In-DOTA-βAla-[*7-14*]BN to the GRP receptor and the fact that high levels of receptors are present on the cell surface of PC-3 cells (B_{max} in the 1×10^4 to 1×10^5 range).[28] Moreover, there is strong evidence for active internalization of the receptor–ligand complex[28] in these cells. Furthermore, the control scrambled peptide shows almost no binding and internalization. Our results confirm the high specific binding and internalization of ^{111}In-DOTA-βAla-[*7-14*]BN peptide in PC-3 cells.

Receptor-mediated cellular uptake kinetics of mixed aggregates ($(C18)_2$DOTA/$(C18)_2$L5-[*7-14*]BN and $(C18)_2$DOTA/$(C18)_2$Peg3000-[*7-14*]BN) were evaluated in a similar fashion. The corresponding mixed aggregates in which the BN peptide was replaced by a scrambled sequence ($(C18)_2$L5-*scr*BN or $(C18)_2$Peg3000-*scr*BN) and aggregates containing only $(C18)_2$DOTA were used as negative controls. Radiolabeling of the aggregates was performed at 2×10^{-4} M concentration. Trace amounts of $^{111}InCl_3$ and up to 100 μCi were added to the aggregate formulation after addition of an equal volume of 0.4 N sodium acetate buffer. Confirmation of incorporation of the radioactive label into the aggregates was obtained by gel filtration. Specific preferential binding to PC-3 cells of mixed aggregates containing the five units of AdOO (L5 spacer) between the BN peptide sequence and the hydrophobic chains was observed (10.3 ± 0.82% at 4 h, Fig. 5B), compared to the same aggregates in which the BN peptide was replaced by a scrambled sequence (5.92 ± 0.78% at 4 h) and to the

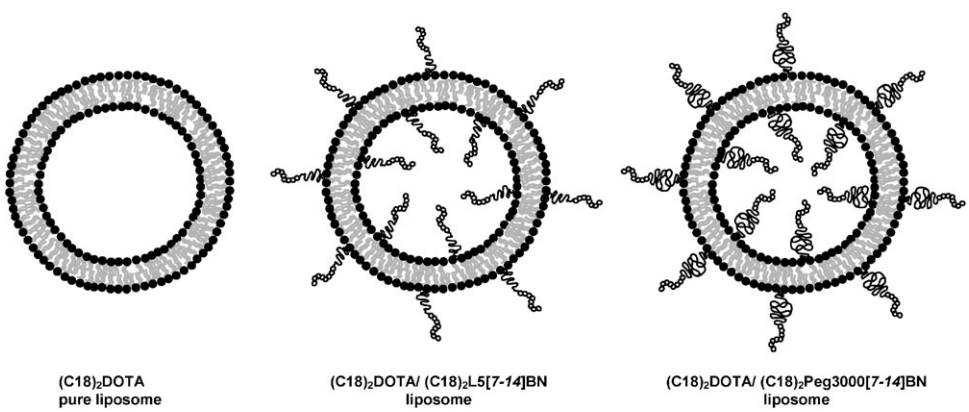

Fig. 4 Schematic view of pure and mixed liposomal aggregates. In all cases, independent of the presence of 10% in peptide monomer in the final composition, liposomes show a hydrodynamic radius, R_h, around 200 nm and bilayer, d, thickness of 4 nm.

$(C18)_2$DOTA aggregates (1.63 ± 0.14% at 4 h). Moreover, binding experiments of mixed aggregates $(C18)_2$DOTA/$(C18)_2$L5[*7-14*]BN were also performed after pre-incubation of cells with the [Tyr^4]-BN blocking reagent. Surprisingly, under these experimental conditions liposomes containing $(C18)_2$DOTA alone show higher binding, with levels comparable to those obtained with the BN containing mixed aggregates (data not shown). We speculated that the hydrophobic residues on the N-terminus of the peptide may be encapsulated in the liposome bilayer during incubation with the cells. This hypothesis was confirmed by fluorescence spectroscopy experiments in which a solution containing $(C18)_2$DOTA aggregates was incubated, under stirring by vortex for 1 min, with a small amount of [Tyr^4]-BN (1 mg). 100 μl of the final solution were separated by gel filtration. The presence in the first gel filtration fractions of a peak at 350 nm, corresponding to the fluorescence emission of the Trp residue in [Tyr^4]-BN, confirms encapsulation of the [Tyr^4]-BN in the aggregates. These results indicate that the [Tyr^4]-BN peptide is unsuitable as receptor blocking reagent in the experiments with aggregates. As shown in Fig. 5B, mixed aggregates show progressively increasing cell associated radioactivity over time (60 min *vs.* 240 min), regardless of which peptide is contained on the surface. Conversely, $(C18)_2$DOTA containing aggregates show no change in the levels of cell associated activity over time. This phenomenon could be related to the presence of the oxoethylene moieties in the L5 linker that, as previously reported for Pegylated liposomes, favors accumulation of aggregates on tumor cells. By using similar binding experiments, we investigated the behavior of $(C18)_2$DOTA/$(C18)_2$Peg3000[*7-14*]BN. The cell associated radioactivity, as shown in Fig. 5C, is lower compared to the values found for the aggregates containing the L5 spacer in the peptide monomer.

We also observed similar values of cell associated radioactivity at all time points investigated for the two aggregates containing either the receptor specific [*7-14*]BN or the scrambled control peptides. For example, at 4 h we found 5.20 ± 0.39% and 4.89 ± 0.35%, respectively. Even if these values are higher compared to the $(C18)_2$DOTA aggregates (1.63 ± 0.14% at 4 h), there is no apparent specificity in binding and internalization due to the bioactive peptide sequence. The presence of the Peg3000 unit on the external liposomal surface may mask the peptide and prevent receptor binding. Moreover, the presence of Peg3000 increases non-specific binding to tumor cells compared to the $(C18)_2$DOTA containing aggregates. These results indicate that aggregates containing a spacer with only five residues of AdOO yield higher accumulation and superior specific interaction with the PC-3 cells compared to aggregates containing the longer Peg3000 spacer. Therefore, the $(C18)_2$DOTA/$(C18)_2$L5[*7-14*]BN mixed aggregate was chosen for experiments in an animal model, using the corresponding aggregate containing the *scr*BN peptide as a negative control.

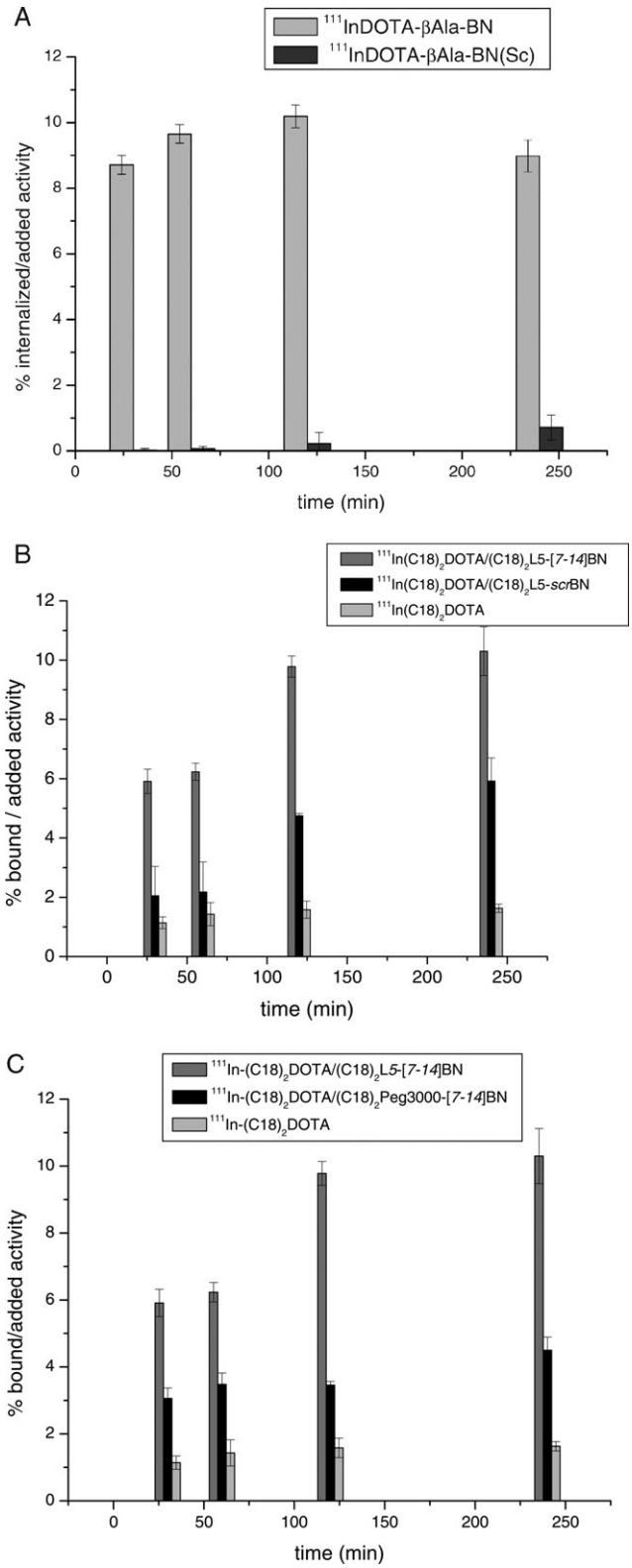

Fig. 5 Binding assays on PC-3 cell lines overexpressing the GRP at 37 °C, at different time points (0.5, 1.0, 2.0 and 4.0 h): (A) binding of ^{111}In-DOTA-βAla-[*7-14*]BN in comparison with ^{111}In-DOTA-βAla-*scr*BN radiolabeled peptides; (B) binding of ^{111}In-labeled aggregates $(C18)_2$DOTA/$(C18)_2$L5-[*7-14*]BN (90 : 10) with respect to the corresponding aggregates in which the BN peptide is replaced by the BN scrambled peptide and to the $(C18)_2$DOTA pure aggregate; (C) binding of ^{111}In-labeled aggregates $(C18)_2$DOTA/$(C18)_2$Peg3000-[*7-14*]BN in comparison with $(C18)_2$DOTA/$(C18)_2$L5-[*7-14*]BN aggregates and with the $(C18)_2$DOTA aggregate.

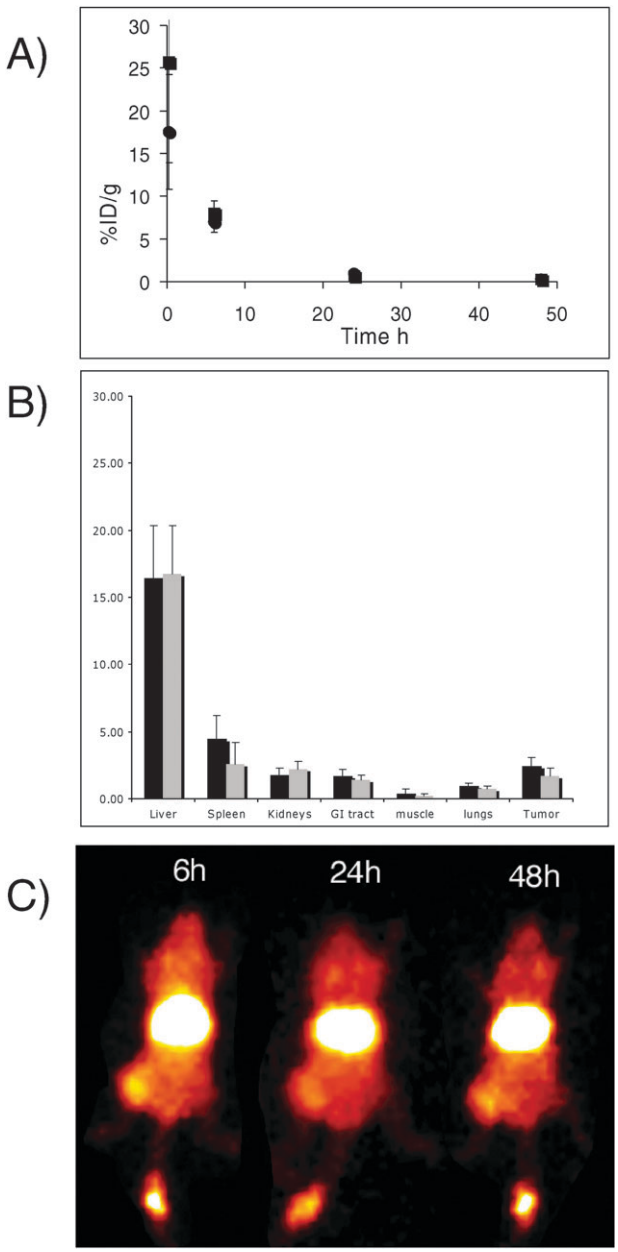

Fig. 6 Animal studies. (A) Blood time activity curve following intravenous injection of ^{111}In-(C18)$_2$DOTA/(C18)$_2$L5-[*7-14*]BN aggregates (squares) and ^{111}In-(C18)$_2$DOTA/(C18)$_2$L5-[*7-14*]*scr*BN aggregates (circles). Error bars = SD. Blood clearance of radioactivity is slow and similar for the two aggregates. (B) Organ biodistribution at 48 h after injection of ^{111}In-(C18)$_2$DOTA/(C18)$_2$L5-[*7-14*]BN aggregates (black bars) and ^{111}In-(C18)$_2$DOTA/(C18)$_2$L5-[*7-14*]*scr*BN aggregates (white bars). Error bars = SD. There is high liver concentration of both aggregates. Uptake in other organs is similar for the two compounds. Higher uptake is observed for ^{111}In-(C18)$_2$DOTA/(C18)$_2$L5-[*7-14*]*scr*BN aggregates in the GRPR positive tumors. (C) Gamma camera images (ventral view) at different times after injection of ^{111}In-(C18)$_2$DOTA/(C18)$_2$L5-[*7-14*]*scr*BN aggregates. Highest uptake is observed in liver although activity in spleen as well as in the tumor located in the right flank are clearly visible over background. Relative concentration of radioactivity in the different organs does remains relatively constant over the 48 h observation period.

2.4 *In vivo* studies

The *in vivo* biological behavior of ^{111}In-(C18)$_2$DOTA/(C18)$_2$L5[*7-14*]BN and ^{111}In-(C18)$_2$DOTA/(C18)$_2$L5[*7-14*]*scr*BN aggregates were evaluated after intravenous injection into GRPR positive tumor bearing mice (PC-3 xenografts). Fig. 6 shows the results of these experiments. Time activity curves of blood radioactivity concentration (Fig. 6a) show fairly long circulation times of the aggregates. This is expected and desired as the intended application of these aggregates is drug delivery that requires high blood concentration of drugs for prolonged periods of time. The observed circulating half-lives of 4–5 h are in agreement with published reports on similar aggregates[29] and are the equivalent of 2–3 day half lives in humans.[30] Biodistribution at 48 h (Fig. 6b) indicates that most radioactivity is in the liver whereas lower levels are obtained in the other organs. Among the other organs, tumors show relatively high concentrations and the GRPR targeting ^{111}In-(C18)$_2$DOTA/(C18)$_2$L5-[*7-14*]BN aggregates show higher concentrations in the PC-3 tumors compared to the scrambled peptide containing control aggregates. There is a slight increase in concentration of the GRPR targeting aggregate in the tumors compared to the control at the 48 h time point evaluated (2.4% ID/g *versus* 1.6% ID/g). The 50% increase in the receptor uptake with respect to the control is similar to the value found for supramolecular aggregates derivatized with CCK8 peptide, in which an average enrichment factor of 48% was observed.[13] This finding justifies further evaluation of this approach. It is noteworthy to point out that the overall accumulation of a potential drug carried by the aggregates to the target tumor is not only dependent on concentration of the aggregate in the tumor at the single time point but is also dependent on aggregate concentration as a function of time. Thus the integral of drug concentration in the tumor *versus* time is likely to benefit greatly from the targeting ability of the liposomes although this aspect needs to be specifically addressed in future experiments. Fig. 6c shows gamma camera images at different times after injection of ^{111}In-(C18)$_2$DOTA/(C18)$_2$L5-[*7-14*]BN containing aggregates. The images confirm the high uptake in liver and spleen and clearly show accumulation in the receptor positive tumors. There is similar contrast between the different organs at the three time points, indicating that the relative differences in concentration of the compound in normal organs and in the tumor is maintained throughout the 48 h observation period.

3. Conclusion

New supramolecular aggregates based on the combination of two amphiphilic synthetic monomers have been prepared and structurally characterized. Even if we have already explored the basic concept to obtain peptide modified supramolecular aggregates, as selective delivery systems, by combining together two amphiphilic monomers, the systems here reported are very innovative both for their chemical composition and for their potential application. The presence of the cyclic chelating agent, DOTA, with only three negative charges, on the most abundant monomer, constrains the liposomal structure of the aggregates. In fact, structural characterization

by SANS and DLS techniques indicates the tendency of the DOTA amphiphilic monomer to form stable liposomes, independent of the presence of 10% in peptide monomer in the final composition. The hydrodynamic radius and bilayer thickness values are around 200 nm and 4 nm, respectively. This structure is different from that observed for similar aggregates previously studied[13] in which DTPAGlu amphiphilic monomer is present, and highly polydisperse aggregates (rod-like micelles, open bilayers and vesicles) were found. This behavior could be explained on the basis of the lower negative charge (−3) of DOTA with respect to DTPAGlu (−5): a decrease of the electrostatic repulsion between the headgroups favours the formation of large and low curvature aggregates such as liposomes.[31]

The presence of [*7-14*] bombesin peptide allows the bombesin receptors, such as the gastrin-releasing peptide receptor (GRPR), to be targeted. These receptors have been found overexpressed by tumor cell lines of several human tumors, including prostate cancers, breast carcinomas, SCLSs and non-SCLSs, renal cell carcinomas and ovarian tumors. *In vitro* and *in vivo* results encourage new studies on the possibility to use these systems as target selective delivery systems of drug and/or imaging probes, in pathologies associated with high expression of bombesin receptors. In fact, *in vitro* data show specific binding of the ^{111}In-(C18)$_2$DOTA/(C18)$_2$L5-[*7-14*]BN containing aggregates in receptor expressing cells, while the presence of a Peg3000 unit on the external liposomal surface could hide the peptide and prevent the receptor binding. *In vivo* experiments using ^{111}In-(C18)$_2$DOTA/(C18)$_2$L5-[*7-14*]BN show the expected biological behavior of aggregates of such size and molecular composition and preliminarily confirm their ability to specifically target and concentrate in receptor expressing xenografts. Further work will delineate to what extent therapeutic efficacy can be increased by such an approach in the animal model currently presented.

4. Experimental

Protected Nα-Fmoc-amino acid derivatives, coupling reagents and Rink-amide *p*-methylbenzhydrylamine MBHA resin were purchased from Calbiochem-Novabiochem (Laufelfingen, Switzerland). The Fmoc-8-amino-3,6-dioxaoctanoic acid (Fmoc-AdOO-OH) was purchased from Neosystem (Strasbourg, France). DOTA(O*t*Bu)$_3$-OH and Lys[DOTA(O*t*Bu)$_3$]-OH derivative were purchased from Macrocycles (Dallas, TX USA). α-(9-Fluorenylmethyloxycarbonyl) amino-ω-carboxy poly(ethylene glycol) (Fmoc-NH-Peg3000-COOH) was purchased by Iris Biotech GmbH (Marktredwitz, Germany). *N*,*N*-dioctadecylsuccinamic acid was synthesized according to literature.[32] [^{111}In]Cl$_3$ was purchased from Mallinckrodt Med. (Petten, The Netherlands). All other chemicals were commercially available by Sigma-Aldrich, Fluka (Buchs, Switzerland) or LabScan (Stillorgan, Dublin, Ireland) and were used as received unless otherwise stated. All solutions were prepared by weight using doubly distilled water. The pH of all solutions was kept constant at 7.4. Preparative HPLC was carried out on a LC8 Shimadzu HPLC system (Shimadzu Corporation, Kyoto, Japan) equipped with a UV lambda-Max Model 481 detector using a Phenomenex (Torrance, CA) C4 (300 Å, 250 × 21.20 mm, 5 μ) column eluted with an H$_2$O/0.1% TFA (A) and CH$_3$CN/0.1% TFA (B) system from 20% to 95% over 25 min at a flow rate of 20 mL min^{-1}. ^{1}H and ^{13}C NMR spectra were recorded using 400 spectrometer Varian (Palo Alto, CA USA). LC-MS analyses were performed by using Finnigan Surveyor MSQ single quadrupole electrospray ionization (Finnigan/Thermo Electron Corporation San Jose, CA). UV measurements were performed on a UV-vis Jasco V-5505 spectrophotometer equipped with a Jasco ETC-505T Peltier temperature controller with a 1 cm quartz cuvette (Hellma).

4.1 Synthesis of (C$_{18}$H$_{37}$)$_2$CONHLys-(DOTA)CONH$_2$ ((C18)$_2$DOTA)

The monomer was synthesized on solid phase using Rink-amide (MBHA) resin (0.85 mmol g^{-1}; 0.2 mmol, 0.235 g) as polymeric support. After the swelling of the resin in 2 mL of dimethylformamide (DMF) for 1 h, the Fmoc protecting group was removed by adding a mixture of piperidine–DMF 30 : 70. The carboxylic group of Fmoc-Lys(Mtt)-OH (0.8 mmol, 0.500 g) was activated by 1 equiv. of benzotriazol-1-yl-oxy-tris(pyrrolidino)phosphonium (PyBop), 1-hydroxybenzotriazole (HOBt) and 2 equiv. of *N*,*N*-diisopropylethylamine (DIPEA) in DMF. The solution was added to the resin and the slurry suspension was stirred for 1 h. The coupling of the lysine residue was performed twice and after filtration, the coupling was checked by the Kaiser colorimetric test. The solution was filtered and the resin washed with three portions of DMF and three portions of dichloromethane (DCM). The 4-methyl-trityl protecting group (Mtt) was removed by treatment of the resin with DCM–tri-isopropylsylane (TIS)–trifluoroacetic acid (TFA) (94 : 5 : 1) mixture stirring for 5 min. This procedure was repeated several times until the solution became colourless. The resin was washed three times with DCM and three times with DMF. DOTA(O*t*Bu)$_3$-OH (2 equiv., 0.252 g) was dissolved in DMF. Two equivalents of O-(7-azabenzotriazol-1-yl)-1,1,3,3-tetramethyluronium (HATU) and 4 equiv. of DIPEA were used to perform the coupling and the reaction was monitored by Kaiser test. Then, after the removal of N-terminal Fmoc protecting group in previous described condition, *N*,*N*-dioctadecylsuccinamic acid (0.4 mmol, 0.249 g) was condensed twice for 1 h in the DMF–DCM (50 : 50) mixture. The lipophilic moiety was activated *in situ* by the standard HOBt–PyBop–DIPEA procedure. The cleavage from the resin and deprotection of the *t*Bu protecting groups were obtained stirring for 2 h in TFA containing 2.5% (v/v) water and 2.0% (v/v) TIS as scavengers at room temperature. The crude product was slowly precipitated at 0 °C by adding water drop-wise. The solid was washed several times with small portions of cold water, and lyophilized. The white solid was recrystalized from MeOH–H$_2$O and recovered in high yield (> 85%). The product was identified by mass spectra (electrospray ionization ESI) and NMR spectroscopy.

(C18)$_2$DOTA: MS (ESI$^+$): *m*/*z* (%): 1134 (100) [M-H$^+$]

^{1}H NMR (CDCl$_3$–CD$_3$OD 50 : 50) chemical shifts δ (CHCl$_3$ as internal standard 7.26) = 4.1 (m, 1H, C*H* Lys α), 3.6 (m, 2H, R$_2$NC*H*$_2$CONH), 3.1 (m, 6H, R$_2$N–C*H*$_2$COOH), 3.0 2H,

CH_2 Lys ε), 3.1 (m, 16 R_2N–$CH_2CH_2NR_2$) 2.4–2.1 (m, 4H, $COCH_2CH_2CO$), 1.7 (m, 2H, CH_2 Lys β), 1.4 (m, 2H, CH_2 Lys δ), 1.3 (m, 2H, CH_2 Lys γ), 1.1 (m, 4H, RCH_2CH_2N), 1.0 (m, 60 CH_2 aliphatic), 0.70 (t, 6H, CH_3).

^{13}C NMR ($CDCl_3$–CD_3OD 50 : 50) chemical shifts δ ($CDCl_3$ as internal standard 77.00) = 174.0 (3, *C*OOH), 172.8, 172.6, 172.1, 163.0 (4 *C*ONH), 54.5 (*C*H Lys α), 53.2 (CH_2COOH), 51.50 (NCH_2CH_2N), 49.7 ($CH_3(CH_2)_{16}CH_2N$), 46.4 ($CH_3(CH_2)_{15}CH_2CH2N$), 38.0 (CH_2 Lys ε), 36.0 (CH_2 Lys β), 32.0 (NCO*C*H2*C*H_2CONH), 31.8 (CH_2 Lys γ), 29.60–27.0 ($CH_3CH_2CH_2(CH_2)_{13}CH_2CH_2N$), 22.57 ($CH_3CH_2$-$CH_2(CH_2)_{15}$), 22.2 ($CH_2$ Lys δ), 13.73 ($CH_3CH_2(CH_2)_{16}$).

4.2 Peptide conjugate synthesis

Peptide syntheses were carried out in solid-phase under standard Fmoc strategy, by using 433A Applied Biosystems automatic synthesizer. Rink-amide MBHA resin (0.78 mmol g^{-1}, 0.5 mmol scale, 0.640 g) was used. The elongations of the [*7-14*]BN and *scr*BN peptides were achieved by sequential addition of Fmoc-AA-OH with PyBOP–HOBt–DIPEA (1 : 1 : 2) as coupling reagents, in DMF in pre-activation mode. The mixture was stirred for 1 h and after filtration. All couplings were performed twice for 1 h, by using an excess of 4 equivalents for the single amino acid derivative. Fmoc deprotections were obtained by 30% solution of piperidine in DMF. Fmoc-AdOO-OH and Fmoc-NH-Peg3000-COOH linkers were coupled manually in DMF by using an excess of 2 equivalents. *N*,*N*-dioctadecylsuccinamic acid coupling was performed as previously described for $(C18)_2$DOTA synthesis.

DOTA-βAla-[*7-14*]BN and DOTA-βAla-*scr*BN: Rt = 19.1 min; MW = 1525 amu; $[M + H^+]$ = 1526.0 amu.

$(C18)_2$L5-[*7-14*]BN and $(C18)_2$L5-*scr*BN: Rt = 22.50 min; MW = 2264 amu; $[M + 2H^+]/2$ = 1133.0 amu.

$(C18)_2$Peg3000-[*7-14*]BN and $(C18)_2$Peg3000-*scr*BN: Rt = 21.9 min; MW = 4544 amu; $[M + 3H^+]/3$ = 1515.7 amu, $[M + 2H^+ + Na^+]/3$ = 1523.0 amu.

4.3 Aggregates preparation

All solutions were prepared by weight, buffering the samples at pH 7.4 by using 0.1 M phosphate buffer. pH was controlled by using pH meter MeterLab PHM 220. In most cases the samples to be measured were prepared from stock solutions. Pure aggregates of $(C18)_2$DOTA and mixed aggregates of $(C18)_2$DOTA/$(C18)_2$L5-[*7-14*]BN and $(C18)_2$DOTA/$(C18)_2$Peg3000-[*7-14*]BN (or aggregates containing their corresponding *scr*BN peptide) were prepared by dissolving the amphiphiles, in a small amount of a methanol–chloroform (50 : 50) mixture, and subsequently evaporating the solvent by slowly rotating the tube containing the solution under a stream of nitrogen. In this way a thin film of amphiphile was obtained. Then the film was hydrated by addition of 0.1 M phosphate buffer (pH = 7.4) solution in the vial and sonicated for 30 min. All mixed aggregates were prepared at 90 : 10 molar ratios between monomer containing the chelating agent and the monomer containing the [*7-14*]BN or *scr*BN peptide. Concentrations of solutions containing peptide surfactant were determined by absorbance measurements. A molar absorptivity (ε_{280}) of 5630 M^{-1} cm^{-1} was used taking into account the contribution from tryptophan present in the primary of the bombesin.[33,34] In all solutions used for SANS investigations, H_2O has been replaced by D_2O in order to minimize the incoherent contribution to the total scattering cross section.

4.4 Small angle neutron scattering (SANS)

Small angle neutron scattering measurements were performed at 25 °C with the KWS2 instrument located at the Heinz Meier Leibtnitz Source, Garching Forschungszentrum (Germany). Neutrons with a wavelength spread $\Delta\lambda/\lambda \leq 0.2$ were used. A two-dimensional array detector at three different wavelengths (W)/collimation(C)/sample-to-detector(D) distance combinations (W_7 Å$C_{8m}D_{2m}$, W_7 Å$C_{8m}D_{8m}$ and W_{19} Å$C_{8m}D_{8m}$), measured neutrons scattered from the samples. These configurations allowed data collection in a range of the scattering vector modulus $q = 4\pi/\lambda\sin(\theta/2)$ between 0.0019 $Å^{-1}$ and 0.179 $Å^{-1}$, where θ is the scattering angle. The investigated systems were contained in a closed quartz cell, in order to prevent solvent evaporation and measurements taken for a period so as to allow ~2 million counts. The obtained raw data were then corrected for background and empty cell scattering. Detector efficiency corrections, radial average and transformation to absolute scattering cross sections $d\Sigma/d\Omega$ were made with a secondary plexiglass standard.[35,36]

4.5 Dynamic light scattering (DLS)

The light scattering setup was composed by a Photocor compact goniometer, a SMD 6000 Laser Quantum 50 mW light source operating at 5325 Å and a PMT and correlator acquired from www.correlator.com.

In DLS, the intensity autocorrelation function $g^{(2)}(t)$ is measured and related to the electric field autocorrelation $g^{(1)}(t)$ by the Siegert relation. The parameter $g^{(1)}(t)$ can be written as the Laplace transform of the distribution of the relaxation rate Γ. Such Laplace transformations were performed using algorithm incorporated in Precision Deconvolve software. From the relaxation rates, the translational diffusion coefficient D may be obtained as[37]

$$D = \lim_{q \to 0} \frac{\Gamma}{q^2} \qquad (2)$$

where $q = 4\pi n_0/\lambda\sin(\theta/2)$ is the modulus of the scattering vector, n_0 is the refractive index of the solution, λ is the incident wavelength and θ represents the scattering angle. Thus D is obtained from the limit slope of Γ as a function of q^2, where Γ is measured at different scattering angles. All the measurements were performed at (25.00 ± 0.05) °C by using a thermostat bath.

4.6 Preparation of the radiotracers

The DOTA-βAla-[*7-14*]BN and DOTA-βAla-*scr*BN radiopeptides were prepared according to Wild *et al.*[38] Briefly, 10 μg of peptide in 250 μL of sodium acetate buffer (0.4 mol L^{-1}, pH 5.0) were incubated with $^{111}InCl_3$ (3 to 5 mCi) for 30 min at 95 °C and then excess of $^{nat}InCl_3 \times 5H_2O$ was added to afford structurally characterized homogenous ligands. Radiolabeling of the aggregates was performed at a final concentration of

2×10^{-4} M. Trace amounts of $^{111}InCl_3$ (100 μCi) were added to 1 mL of the aggregates and sodium acetate buffer (0.4 mol L^{-1}, pH 5.0) was added to reach a final volume of 2 mL. The mixture was incubated for 30 min at 90 °C. Confirmation of incorporation of the label into the aggregates was obtained by gel filtration on Sephadex G-50 pre packed columns (Pharmacia Biotech).

4.7 *In vitro* studies

PC-3 cells were seeded into 6-well plates wherein they remained overnight ($0.8–1.0 \times 10^6$ cells per well). On the day of the experiment the medium was removed, the cells were washed twice with fresh medium (DMEM with 1% fetal bovine serum, pH 7.4) and incubated for 1 h at 37 °C. Internalization experiments of the ^{111}In-labeled peptides were performed as indicated in the literature.[39] Approximately 0.08 μCi of $^{111/nat}$In-labeled peptide (0.25 pmol) were added to the medium and the cells were incubated (in triplicates) for 0.5, 1, 2 and 4 h at 37 °C, 5% CO_2. A 1000 fold excess of [Tyr^4]-BN was used to determine non-specific internalization. At each time point the internalization was stopped by removing the medium followed by washing the cells with ice-cold solutions of phosphate-buffered saline (PBS, pH 7.4). Cells were then treated for 5 min (twice) with glycine buffer (0.05 mol L^{-1} glycine solution, pH adjusted to 2.8 with 1 mol L^{-1} HCl) to distinguish between cell surface-bound (acid releasable) and internalized (acid resistant) radioligand. Finally, the cells were detached from the plates by incubating with 1 mol L^{-1} NaOH for 10 min at 37 °C. An amount of 0.5 μCi (100 μL) per well of $^{111/nat}$In-labeled aggregates to a final concentration of 2×10^{-4} M were added to the medium and the cells were incubated (in triplicates) for 0.5, 1, 2 and 4 h at 37 °C, 5% CO_2. Afterwards, the binding buffer was aspirated and the cells were washed twice with ice-cold phosphate-buffered saline (PBS, pH 7.4); this represented the unbound fraction. The cells were then collected with 1 N NaOH; this corresponded to the bound fraction. The calculations of the *in vitro* experiments were done by measuring the radioactivity of each collected fraction in a γ-counter (Cobra II; Packard Instrument Co.) related to the standards.

4.8 *In vivo* studies

Animal experiments were carried out on 6 week old female CD1 nude mice (Charles River Italia). Mice bearing xenografts of PC-3 cells were generated as previously described.[13] Briefly, 100 μL of the cell suspensions at a density of 2–3 10^7 mL^{-1} in PBS were injected in the flank of mice (weight 17–23 g). Biodistribution and imaging experiments were performed two weeks after implanting cells (tumor sizes were between 0.5 and 1 g). Procedures involving animals and their care were in conformity with institutional guidelines that comply with national and international laws and policies. Approximately 100 μCi of ^{111}In-labeled aggregate preparation ($(C18)_2$DOTA/$(C18)_2$L5-[*7-14*]BN and the corresponding aggregates in which the BN peptide is replaced by the scrambled peptide) were injected into the lateral tail vein of each mouse ($n = 5$). Imaging was performed at different times after injection, following administration of an intraperitoneal anesthetic on a clinical gamma camera equipped with a medium energy collimator. Venous orbital sinus samples were also collected at different times to obtain blood time activity curves. The animals were killed 48 h after injection, imaged and subsequently dissected in order to quantitatively determine organ concentrations of radioactivity by weighing and counting each dissected organ. Dilutions of the injected compound were simultaneously counted for accurate determination of the injected dose. The relative amount of radioactivity in the organs was calculated and expressed as a percentage of the injected dose/gram tissue (%ID/g) normalized to a 20 g mouse.

Acknowledgements

We thank Prof. Helmut Maecke, University Hospital Basel, Switzerland for the helpful discussions and suggestions. We are indebted to EMIL, European Molecular Imaging Laboratories, for financial support. Some of us (LP, GM, AR) wish to thank the Forschungszentrum Jülich for provision of beam time.

References

1 V. P. Torchilin, *Eur. J. Pharm. Biopharm.*, 2009, **71**, 431–444.
2 W. T. Al-Jamal and K. Kostarelos, *Nanomedicine (London, UK)*, 2007, **2**(1), 85–98.
3 V. P. Torchilin, *Nat. Rev. Drug Discovery*, 2005, **4**, 145–160.
4 V. P. Torchilin, *J. Controlled Release*, 2001, **73**, 137–172.
5 M. Ferrari, *Nat. Rev. Cancer*, 2005, **5**, 161–17.
6 T. M. Allen, *Nat. Rev. Cancer*, 2002, **2**, 750–763.
7 W. J. M. Mulder, G. J. Strijkers, K. C. Briley-Saebo, J. C. Frias, J. G. S. Aguinado, E. Vudic, V. Amirbekian, C. Tang, P. T. K. Chin, K. Nicolay and Z. A. Fayad, *Magn. Reson. Med.*, 2007, **58**, 1164.
8 A. Accardo, D. Tesauro, P. Roscigno, E. Gianolio, L. Paduano, G. D'Errico, C. Pedone and G. Morelli, *J. Am. Chem. Soc.*, 2004, **126**, 3097–3107.
9 A. Accardo, D. Tesauro, G. Morelli, E. Gianolio, S. Aime, M. Vaccaro, G. Mangiapia, L. Paduano and K. Schillen, *JBIC, J. Biol. Inorg. Chem.*, 2007, **12**, 267–276.
10 D. Tesauro, A. Accardo, E. Gianolio, L. Paduano, J. Teixeira, K. Schillen, S. Aime and G. Morelli, *ChemBioChem*, 2007, **8**, 950–955.
11 M. Vaccaro, G. Mangiapia, L. Paduano, E. Gianolio, A. Accardo, D. Tesauro and G. Morelli, *ChemPhysChem*, 2007, **8**, 2526–2538.
12 A. Accardo, D. Tesauro, G. Mangiapia, C. Pedone and G. Morelli, *Biopolymers*, 2007, **88**, 115–121.
13 A. Accardo, D. Tesauro, L. Aloj, L. Tarallo, C. Arra, G. Mangiapia, M. Vaccaro, C. Pedone, L. Paduano and G. Morelli, *ChemMedChem*, 2008, **3**, 594–602.
14 J. F. Battey, J. M. Way, M. H. Corjay, H. Shapira, K. Kusano, R. Harkins, J. M. Wu, T. Slattery, E. Mann and R. I. Feldman, *Proc. Natl. Acad. Sci. U. S. A.*, 1991, **88**, 395–399.
15 Z. Fathi, M. H. Corjay, H. Shapira, E. Wada, R. Benya, R. Jensen, J. Viallet, E. A. Sausville and J. F. Battey, *J. Biol. Chem.*, 1993, **268**, 5979–5984.
16 S. R. Nagalla, B. J. Barry, K. C. Creswick, P. Eden and J. T. Taylor, *Proc. Natl. Acad. Sci. U. S. A.*, 1995, **92**, 6205–6209.
17 E. Wada, J. Way, H. Shapira, K. Kusano, A. M. Lebacq-Verheyden, D. Coy, R. Jensen and J. Battey, *Neuron*, 1991, **6**, 421–430.
18 R. Markwalder and J. C. Reubi, *Cancer Res.*, 1999, **59**, 1152–1159.
19 M. Gugger and J. C. Reubi, *Am. J. Pathol.*, 1999, **155**, 2067–2076.
20 A. Fleischmann, B. Waser and J. C. Reubi, *Cell Oncol.*, 2007, **29**, 421–433.
21 C. J. Smith, W. A. Volkert and T. J. Hoffman, *Nucl. Med. Biol.*, 2005, **32**, 733–740.

22 B. E. Rogers, H. M. Bigott, D. W. McCarthy, D. Della Manna, J. Kim, T. L. Sharp and M. J. Welch, *Bioconjugate Chem*., 2003, **14**, 756–763.
23 J. J. Parry, T. S. Kelly, R. Andrews and B. E. Rogers, *Bioconjugate Chem*., 2007, **18**, 1110–1117.
24 A. Al-Nahhas, Z. Win, T. Szyszko, A. Singh, C. Nanni, S. Fanti and D. Rubello, *Anticancer Res*., 2007, **27**(6B), 4087–4094.
25 T. M. Allen, C. Hansen, F. Martin, C. Redemann and A. Yau-Young, *Biochim. Biophys. Acta, Biomembr*., 1991, **1066**(1), 29–36.
26 W. C. Chang and P. D. White, *Fmoc Solid Phase Peptide Synthesis*, Oxford Univ Press, 2000.
27 F. Hu, C. S. Cutler, T. Hoffman, G. Sieckman, W. A. Volkert and S. S. Jurisson, *Nucl. Med. Biol*., 2002, **29**, 423–430.
28 H. Reile, P. E. Armatis and A. V. Schally, *Prostate (New York, United States)*, 1994, **25**, 29–38.
29 D. S. Alberts, F. M. Muggia, J. Carmichael, E. P. Winer, M. Jahanzeb, A. P. Venook, K. M. Skubitz, E. Rivera, J. A. Sparano, N. J. Dibella, S. J. Stewart, J. J. Kavanagh and A. A. Gabizon, *Semin. Oncol*., 2004, **31**, 53–90.
30 K. Schneider, J. Oltmanns and M. Hassauer, *Regul. Toxicol. Pharmacol*., 2004, **39**(3), 334–347.
31 M. Vaccaro, A. Accardo, D. Tesauro, G. Mangiapia, D. Löf, K. Schillen, O. Soderman, G. Morelli and L. Paduano, *Langmuir*, 2006, **22**, 6635–6643.
32 L. Schmitt, C. Dietrich and R. Tampe, *J. Am. Chem. Soc*., 1994, **116**, 8485–8491.
33 H. Edelhoch, *Biochemistry*, 1967, **6**, 1948–1954.
34 C. N. Pace, F. Vajdos, L. Fee, G. Grimsley and T. Gray, *Protein Sci*., 1995, **4**, 2411–2423.
35 T. P. Russell, J. S. Lin, S. Spooner and G. D. Wignall, *J. Appl. Crystallogr*., 1988, **21**(6), 629–38.
36 G. D. Wignall and F. S. Bates, *J. Appl. Crystallogr*., 1987, **20**(1), 28–40.
37 B. J. Berne and R. Pecora, *Dynamic Light Scattering with Applications to Chemistry, Biology and Physics*, John Wiley & Sons, New York, 1976.
38 A. Heppeler, S. Froidevaux, H. R. Maecke, E. Jermann, M. Behe, P. Powell and M. Hennig, *Chem.–Eur. J*., 1999, **5**, 1974–1981.
39 H. Zhang, J. Chen, C. Waldherr, K. Hinni, B. Waser, J. C. Reubi and H. R. Maecke, *Cancer Res*., 2004, **64**, 6707–15.